

**DETERMINATION OF AEROSOL PHYSICAL PARAMETERS IN THE DEEP LAYERS OF THE SATURN'S ATMOSPHERE.** A. S. Ovsak<sup>1</sup>, <sup>1</sup>Main Astronomical Observatory of the NAS of Ukraine, Zabolotnoho Street 27, Kyiv, 03143, [ovsak@mao.kiev.ua](mailto:ovsak@mao.kiev.ua).

**Introduction:** For the first time, reliable physical parameters of aerosol particles in the upper part of Saturn's atmosphere were determined in [1] from the analysis of polarimetric measurements data from the near-equatorial part of the disk of giant planet. It was been confirmed by the results of [7] and [18]. The values of those parameters are: the effective radius  $r_{eff} = 1.4 \mu m$ , the dispersion  $v_{eff} = 0.07$  and the real part of the refractive index  $n_r = 1.44$  for recalculation on a modified gamma particle-size distribution function.

Further, possible values of  $r_{eff}$  on the numerous altitudinal levels in the different latitudinal belts of both hemispheres of the giant planet were determined in [3, 6, 8, 10, 15–17, 21]. All they were calculated using a various analysis techniques and models of vertical structure of the atmosphere. So, the value of  $r_{eff}$  were determined from  $\leq 0.1 \mu m$  in the stratospheric haze up to  $\geq 2.25 \mu m$  in the convective clouds rising from the deep layers of the troposphere.

In [12], author has analyzed the data of spectrophotometric measurements of Saturn's disk [5]. As a result, a dependence on the pressure of the aerosol scattering component  $\tau_{eff}^a(\ln P)$  of the optical depth of the giant planet's atmosphere is determined in the methane absorption bands at wavelengths  $\lambda = 619, 727, 842, 864$  and  $887$  nm. At certain altitude levels in the depth of the atmosphere, the indicated dependence shows the features that possibly reflect changes in the physical characteristics of aerosol. Therefore, the aim of this work to determine the possible values of the physical parameters of aerosol particles at altitudinal levels with the features noted above.

**Analysis method:** The analysis of the  $\tau_{eff}^a(\ln P)$  dependence in this study is based on the same technique for determining the parameters of the size distribution function of aerosol particles in the deep layers of the giant planet's atmosphere that was already use in [11]. For this reason, we use the values of the aerosol volume scattering coefficient  $\sigma_a(P_i)$  calculated at couple of altitudinal segments of the atmosphere in different methane absorption band. Detailed description of the algorithm for determining these coefficients is given in [13]. It will be note that the reliable data of the temperature dependence on the pressure in the atmosphere is critically important for the mentioned algo-

rithm. Thus stressed here, we obtained the temperature versus pressure dependence in Saturn's atmosphere by combining the results of [3] and [9] and interpolated them to the deep layers of the atmosphere with consideration of its adiabatic properties.

After studying the results of [12, 14], we selected the altitudinal segments of Saturn's atmosphere (see Fig.1)

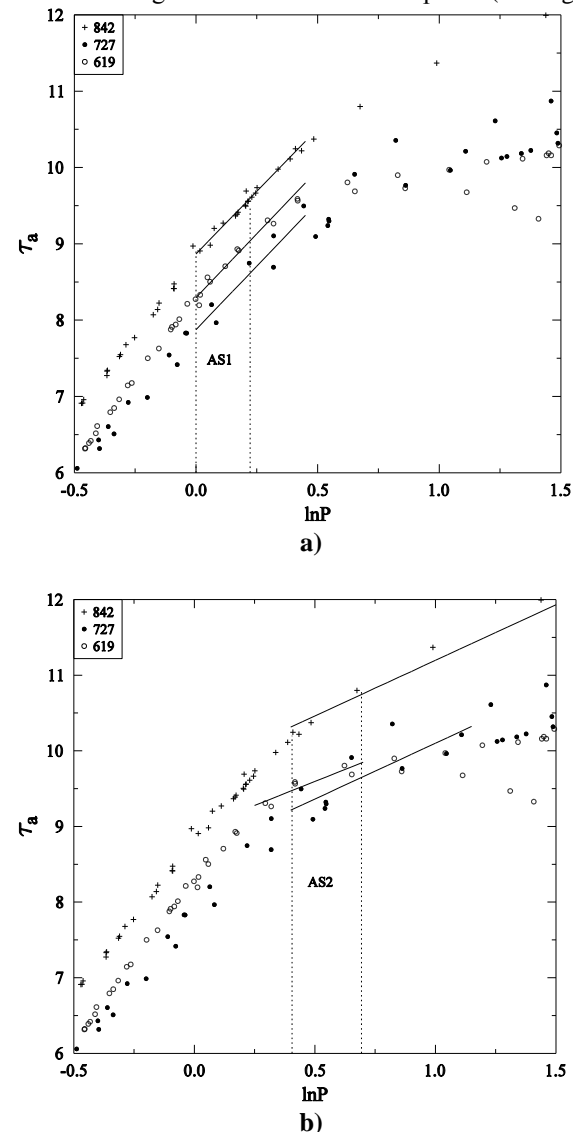


Fig.1 The dependence of  $\tau_{eff}^a$  on the pressure logarithm in the methane absorption bands at  $\lambda = 619, 727$  and  $842$  nm formed from the data of [12]. The altitudinal segments AS1 and AS2 are shown.

with pressure ranges of 1.0–1.25 bar (AS1) and 1.5–2.0 bar (AS2) for processing. The reasons for this choice are the following: 1) at the outer boundary of both segments the tilt angle of the  $\tau_{eff}^a(\ln P)$  dependence simultaneously changes for all methane absorption bands; 2) within both segments, there are no significant clouds thickening or rarefaction. That allows one to assume their relative uniformity and perform the linear approximation of the points on the  $\tau_{eff}^a(\ln P)$  dependences calculated in each of the absorption band. Similar to [11], calculated points of the  $\tau_{eff}^a(\ln P)$  dependences at the altitudinal segments AS1 and AS2 were approximated using the linear regression method. The ratio of the spectral values of the coefficients  $\sigma_a(\lambda_i)/\sigma_a(\lambda_j)$  was calculated from the tilt angles between the horizontal axis and the approximation intervals obtained separately in the each methane absorption band for both altitudinal segments AS1 and AS2. It should be emphasized that ‘experimental’ values  $\sigma_a(\lambda_j)$  not reduced to the one wavelength are obtained using the parameters of aerosol particles in the upper part of Saturn’s atmosphere. To determine the possible values of aerosol parameters, following relation will be true to a certain accuracy:

$$\sigma_a(\lambda_i)/\sigma_a(\lambda_k) \approx \sigma_0(\lambda_i)/\sigma_0(\lambda_k), \quad (1)$$

where  $\sigma_a(\lambda_i), \sigma_a(\lambda_k)$  – the values of the aerosol volume scattering coefficient calculated from the experimental data in absorption bands with centers at wavelengths  $\lambda_i, \lambda_k$ , and  $\sigma_0(\lambda_i), \sigma_0(\lambda_k)$  are the values of the volume scattering coefficient of the unit part of the model medium containing polydispersal assembly of uniform spherical aerosol particles calculated at the wavelengths  $\lambda_i, \lambda_k$  of the cores of mentioned above absorption bands. Then, by varying the parameters of particle size distribution function and using the model calculations of the  $\sigma_0(\lambda_i)$  and  $\sigma_0(\lambda_k)$  values, we can select those values of the parameters at which relation (1) is the closest to an identity for all combinations of coefficients  $\sigma_0(\lambda_i)$  at the altitudinal segment under study.

**Results:** The analysis at AS1 segment shows the value of  $n_r = 1.44$ , it is similar to the value in upper part of Saturn’s atmosphere, and the effective radius of cloud particles grows up to  $1.85 \mu m$ . There is an 3.5% decrease of value  $n_r$  at the segment AS2 and the effective radius of aerosol particles grows up to  $2.2–2.4 \mu m$ .

The values of the  $r_{eff}$  of aerosol particles determined in the present study closely agree with the results of [6, 17, 21]. There is also an exceptionally good agreement with the  $r_{eff}$  values obtained in [16] for the altitudinal layers in the atmosphere of Saturn’s southern hemisphere, with pressure close to the segments AS1 and AS2. Existence of ammonia and water in Saturn’s atmosphere was been predicted long ago [2]. But presence of both these substances reliably confirmed only in [19, 20] at the region of the Great Storm of 2010–2011. As it’s known, water and ammonia mixed easily and forms ammonium hydroxide  $NH_4OH$ . The melting temperature of its 35% water solution  $T_w \approx 181$  K [4]. According to results [3, 9], the temperature in Saturn’s atmosphere increases with depth to near 180 K at the AS2 altitudinal segment. Thus, one can assume a change the phase state of cloud particles in the depth of Saturn’s atmosphere, if those clouds consisting the ammonia hydroxide is at sufficient concentration. This process can explains the revealed decrease of  $n_r$  value of aerosol. Thus, a probable component of clouds in the deep layers of the atmosphere of Saturn may be an ammonium hydroxide.

**Conclusion:** Using the data of spectral measurements of the geometric albedo, the possible values of the physical parameters of aerosol in the deep layers of Saturn’s atmosphere were determined.

**References:** [1] Bugaenko O. I. et al. (1975) *Astron. Vestn. (on russian)*, 9, 13–21. [2] Atreya S. K. and Wong A. S. (2005) *Sp. Sc. Rev.*, 116, 121–136. [3] Fletcher, L. N. et al. (2017) *Nature Astronomy*, 1, 765–770. [4] Hildenbrand D. L. and Giauque W. F. (1953) *J. Am. Chem. Soc.*, 75, 2811–2818. [5] Karkoschka E. (1994) *Icarus*, 111, 967–982. [6] Karkoschka E. and Tomasko M. G. (2005) *Icarus*, 179, 195–221. [7] Kawata K. (1978) *Icarus*, 33, 217–233. [8] Kerola D.X. et al. (1997) *Icarus*, 127, 190–212. [9] Lindal G. F. (1992) *Astron. Journ.*, 103, 967–982. [10] Muñoz O. et al. (2004) *Icarus*, 169, 413–428. [11] Morozhenko A.V. and Ovsak A.S. (2017) *Kinemat. Phys. Celest. Bodies*, 33, 173–181. [12] Ovsak A.S. (2018) *Kinemat. Phys. Celest. Bodies*, 34, 37–51. [13] Ovsak A. S. (2015) *Kinemat. Phys. Celest. Bodies*, 31, 197–204. [14] Ovsak A.S. (2018) *LPS XXXIX*, Abstract #1069. [15] Pérez-Hoyos S. et al. (2005) *Icarus*, 176, 155–174. [16] Roman M. T. et al. (2013) *Icarus*, 225, 93–110. [17] Sánchez-Lavega A. et al. (2007) *Icarus*, 187, 510–519. [18] Santer R. and Dollfus A. (1981) *Icarus*, 48, 496–518. [19] Sromovsky L.A. et al. (2013) *Icarus*, 226, 402–408. [20] Sromovsky L.A. et al. (2016) *Icarus*, 276, 141–162. [21] Temma T. et al. (2005) *Icarus*, 175, 464–489.